Comparison of spiral-in/out and spiral-out BOLD fMRI at 1.5 and 3 T

Alison R. Preston[a], **Moriah E. Thomason**[b], **Kevin N. Ochsner**[a], **Jeffrey C. Cooper**[a], **Gary H. Glover**[b,c,*]

[a]Department of Psychology, Stanford University, Stanford, CA 94305, USA

[b]Neurosciences Program, Stanford University, Stanford, CA 94305, USA

[c]Department of Radiology, Lucas MR Center, Stanford University, Stanford, CA 94305, USA

Abstract

Spiral-in/out functional magnetic resonance imaging (fMRI) methods acquire one image before the echo time (TE) and a second image after TE during each scan. Weighted combination of the two images provides a time series with reduced susceptibility dropout in frontal and medial temporal regions as well as increased signal-to-noise ratio (SNR) in regions of uniform cortex. In this study, task activation with the spiral-in/out method was compared to that with conventional spiral-out acquisitions at two field strengths (1.5 and 3.0 T) using episodic memory encoding, verbal working memory, and affective processing tasks in eight human volunteers. With the conventional spiral-out sequence, greater signal dropout is observed in lateral and medial prefrontal, amygdalar, and medial temporal regions at 3 T relative to 1.5 T, whereas such dropout at 3 T is reduced or mitigated with the spiral-in/out method. Similarly, activation volumes for frontal, amygdalar, and medial temporal regions are reduced for spiral-out acquisitions relative to spiral-in/out, and this difference is more apparent at 3 T than at 1.5 T. In addition, significant regionally specific increases in Z scores are obtained with the spiral-in/out sequence relative to spiral-out acquisitions at both field strengths. It is concluded the spiral-in/out sequence may provide significant advantages over conventional spiral methods, especially at 3 T.

Keywords

Spiral-in/out; BOLD; fMRI

Introduction

Functional magnetic resonance imaging (fMRI) uses a T2*-weighted acquisition sequence to develop Blood Oxygen Level Dependent (BOLD) contrast (Bandettini et al., 1992; Kwong et al., 1992; Ogawa et al., 1990). If the transverse magnetization decays exponentially with relaxation time T2*, the BOLD contrast is maximized when the echo time TE is made comparable to T2*. However, such long TEs sensitize the acquisition to the

*Corresponding author. Department of Radiology, Lucas MR Center, Stanford University School of Medicine, 1201 Welch Road, Stanford, CA 94305-5488. Fax: +1-650-723-5795. gary@s-word.stanford.edu (G.H. Glover).

deleterious effects of macroscopic susceptibility-induced field gradients (SFGs) generated near air–tissue interfaces such as in orbital frontal and medial temporal regions. The resulting signal dropouts from intravoxel dephasing limit the applicability of fMRI for many studies that attempt to probe such cortical areas. Moreover, SFGs increase linearly with field strength, so that the dropout regions tend to be larger at 3 T than at 1.5 T because TE is generally reduced proportionately with T2* to maintain constant BOLD sensitivity in uniform brain [T2* ~ 65 ms/50 ms at 1.5 T/3.0 T, respectively (Kruger et al., 2001; Kastrup et al., 2001], which is less than a factor of 2. Thus, one can question whether the nominal twofold increase in signal-to-noise ratio (SNR) at 3 T relative to 1.5 T is beneficial for fMRI when compromised regions are involved.

This question was addressed in a recent study comparing conventional spiral scans obtained at 1.5 and 3 T using visual perception, spatial working memory (WM), and affective processing tasks (Krasnow et al., 2003). It was found that at 3 T, activation volumes were increased significantly in striate and extrastriate regions (visual task) and in frontal and parietal regions (WM task), but not in amygdala (affective task) in comparison with results at 1.5 T. In fact, signal dropout in the amygdala was observed to be greater at 3 T (12%) than at 1.5 T (9%). Other studies have also examined field strength comparisons, but only in primary visual and motor sensory areas for which signal dropout is not a concern (Gati et al., 1997; Kruger and Glover, 2001; Kruger et al., 2001; Turner et al., 1993; Yang et al., 1999). With the exception of Turner's work wherein superlinear increases in SNR were observed, these studies generally concluded that the BOLD signal scales approximately linearly with field strength as expected from the SNR increases in uniform brain.

Recently, spiral-in/out (termed "spiral-io" here) methods were introduced as a means to increase the SNR and BOLD contrast-to-noise ratio (CNR) in uniform brain regions as well as to reduce the signal loss in regions compromised by SFGs (Glover and Law, 2001). With conventional spiral methods ("spiral-out"), the k-space trajectory starts at the center of k-space at time TE and spirals outward along an Archimedian or other curve until the maximum radius in k-space is achieved according to the desired resolution. By comparison, the spiral-io trajectory starts at the maximum radius in k-space and spirals inward to the k-space origin, which is reached at time TE. Data gathered during this traversal is reconstructed to form a "spiral-in" image. The trajectory then reverses and spirals out as would normally occur for a conventional spiral acquisition, and a second (spiral-out) image is acquired. Previously, it was found that the spiral-in image can have increased signal and BOLD contrast relative to the spiral-out image in regions compromised by SFGs, and that the two images could be combined using weighted averaging to provide increased SNR and BOLD CNR in uniform brain regions (Glover and Law, 2001). Cognitive tasks that recruit brain regions affected by SFG-induced dropout are likely to benefit from spiral-io acquisition methods.

In the current study, we compare spiral-io and spiral-out acquisitions at 1.5 and 3 T during episodic memory encoding, verbal working memory, and affective processing tasks that are known to recruit medial temporal, frontal, and amygdalar regions. Using a spiral-io sequence, eight normal volunteers were scanned while performing four tasks during consecutive sessions on 1.5- and 3-T scanners. The spiral-out data were extracted from the

spiral-io data and processed identically to the combined spiral-io data to allow a comparison of spiral-io vs. spiral-out acquisitions. The same dual-path processing was applied for both field strengths. Activation volumes were quantified using both ROI (region of interest) and global activation masking, and signal dropout and Z scores were assessed using anatomical ROIs defining cortical regions relevant for each task.

This report explicitly excludes a comparison of spiral-in acquisitions with either spiral-out or spiral-io acquisitions. In a related study comparing methods of combining spiral-in and spiral-out time series (Glover and Thomason, in press), it was shown that in many brain regions the spiral-in acquisition results in activation volumes that are reduced compared to those obtained with the conventional spiral-out method. Specifically, that study demonstrated for data from the letters task described here that the spiral-in activation volumes were 80% of those for the spiral-out acquisition.

The explanation for reduced effectiveness of spiral-in relative to spiral-out acquisitions was described briefly in Glover and Thomason (in press) and is elaborated here. For an exponential decay of transverse magnetization, the BOLD sensitivity is proportional to the echo time, and at first glance it would seem that the -in and -out methods should have the same BOLD sensitivity since they share a common TE at $k = 0$. It is true that the two methods yield nearly identical whole-brain contrast and signal intensity in uniform regions. However, for regions of the image that are small compared to the field of view (FOV), such as is generally the case with cortical activation volumes, the higher spatial frequencies become important to the signal definition, and this results in an "effective" echo time to maximize the signal that is longer than TE for spiral-out readout and shorter than TE for the spiral-in trajectory (Glover and Law, 2001). Accordingly, the spiral-in acquisition generally has reduced BOLD sensitivity relative to spiral-out methods in uniform regions. Therefore, it was concluded that the spiral-in method alone is not a viable alternative to spiral-out methods despite its attractiveness with respect to reduced sequence duration and concomitantly increased scan time efficiency, and thus a further spiral-in comparison was not performed in this study.

Materials and methods

Tasks

Four tasks were chosen to activate brain regions known to be problematic for fMRI because of SFGs: lateral prefrontal cortex (LPFC), medial temporal lobe (MTL), ventral medial prefrontal cortex (VMPFC), and amygdala. The order of the four functional scans was randomized across the subjects and between field strengths for the same subject.

Scenes task

The scenes task utilized episodic memory encoding to activate regions in the MTL (Gabrieli et al., 1997; Stern et al., 1996). Subjects viewed color pictures of indoor and outdoor scenes for 3 s and were asked to classify them as indoor or outdoor. There were two types of blocks, novel scenes and repeated scenes. During novel blocks, subjects saw eight unique scenes (four indoor, four outdoor), which appeared once each during the experiment. During

repeated blocks, subjects saw one indoor and one outdoor scene, each repeated four times during a block. Repeated blocks were identical for a given field strength with the same two scenes used for all repeated blocks. During the scan session, there were a total of six repeated and six novel blocks that occurred in a random order, with each block having a duration of 24 s. Different sets of novel scenes were used as stimuli at the different field strengths for each subject.

Letters task

A version of the Sternberg paradigm using letter stimuli was employed as a test of verbal working memory that is known to engage LPFC (Smith and Jonides, 1997). Following a fixation cross, subjects viewed a target set of five letters, then after a brief delay viewed a sixth probe letter that was either a member of the target set (match) or was different from all letters in the target set (nonmatch). Subjects were asked to classify each probe stimulus as either a match or nonmatch response. In this standard, delay-match-to-sample task, two types of delays were used. During experimental blocks, the probe stimuli appeared 3100 ms after the presentation of the target set. During control blocks, the delay between the target and probe stimuli was only 100 ms. The duration of experimental and control blocks was 24 s, with each block containing four, 6-s target-probe trials. During a scan session, a total of eight experimental and eight control blocks were presented in a random order.

Photos task

The photos task and the film task described below are exemplars of tasks known to activate both VMPFC and amygdala (e.g. Lane et al., 1997; Ochsner and Feldman Barrett, 200; for review, see Ochsner et al., 2002). In the photos task, subjects passively viewed six blocks of negative and six blocks of neutral images presented in pseudorandom order. Photo blocks were separated by blocks of fixation crosses, and contained either neutral (e.g., a chair) or aversive (e.g., injured body) photos taken from the International Affective Picture System (Lang et al., 1993) intermixed with either neutral or fear faces. All blocks lasted 18 s. Two different matched sets of images were selected and presented in counterbalanced order across scanners.

Film task

In this task, subjects passively viewed a 2-min video with two 30-s negative segments and two 30-s neutral segments presented in an ABAB design. Two matched video stimuli were prepared and presented in counterbalanced order across scanners so that subjects did not view the same film twice. Each video used one negative segment from a film of a surgical knee amputation (Gross, 1998), and a second from a film of a sheep slaughterhouse. Neutral film segments were drawn from a documentary video about national parks.

Subjects

Eight normal right-handed volunteers (age 19–42, mean 28.5 ± 8.8 years; 6 males, 2 females) were enrolled in the study after giving informed consent in accordance with a protocol approved by the Stanford Institutional Review Board. Each subject was scanned on 1.5- and 3.0-T scanners within the same day, with the magnet order counterbalanced across

subjects. Because of technical difficulties, data were not collected for one subject during the letters task on the 1.5-T scanner, and that subject's data were excluded from the letter task analysis at both fields. After analysis of the scenes task, a different subject's results were deemed unreliable, as activation was negligible for the 3-T scan compared to that from the 1.5-T scan and statistically inconsistent with that from the other seven subjects, and his results were also excluded for both field strengths for that task. Thus, the final analyses utilized seven subjects for the scenes and letters tasks, and eight for the photos and film tasks.

Acquisitions

All imaging data were acquired with 1.5- and 3-T scanners configured with identical gradient characteristics (GE Signa, Milwaukee, WI; rev CNV3 and VH3.8, respectively). On each scanner, the manufacturer's head coil was equipped with a backprojection screen and first surface mirror for presentation of visual stimuli, and the subject's head was thoroughly padded in the coil to reduce bulk head motion. T2-weighted FSE scans were obtained for anatomic reference (TR/TE/ETL = 68 ms/4000 ms/12; 25, 4-mm/skip 1-mm slices, FOV = 24 cm, 192×256 matrix), and 3D IR-prep FSPGR scans were acquired for volume reformation (TR/TE/TI/FA = 9.7 ms/2.3 ms/300 ms/15; 124, 1.4-mm slices; 192×256 matrix). An automated high-order shimming method based on spiral acquisitions was employed to reduce B_0 heterogeneity (Kim et al., 2002).

Functional acquisitions used TR 2000 ms, FOV 24 cm, BW $\pm$ 100 kHz, TE 40 ms/30 ms and FA 90/80° at 1.5 and 3 T, respectively. Twenty-five, 4-mm slices were acquired with an oblique axial scan plane and 1-mm interslice skip. A total of 192 time frames were acquired for scenes and letter tasks, 225 frames for the photos task and 62 frames for the film task. The spiral-in and spiral-out trajectories were identical except for time orientation and used a single-shot, slew-rate limited, Archimedian design with 64×64 matrix (Glover, 1999b). A spectral–spatial RF pulse was used to excite only the water line (Meyer et al., 1990) because artifacts were otherwise generated in the spiral-in image from the off-resonant lipid components in the subcutaneous fat (the high spatial frequency components of the spiral-in acquisition were gathered before the fat signal decayed away sufficiently). Following the functional scan, spiral-in and spiral-out images were automatically reconstructed on the scanner's host computer using gridding (with the calculated trajectories) and FFTs. Linear shim corrections for each slice were applied during reconstruction using individual field maps obtained during the scan (Glover and Lai, 1998b), and corrections were also performed for concomitant field effects (King et al., 1999).

For each scan, two time series of images were obtained. The spiral-io time series were generated by adaptive combination of the spiral-in and spiral-out data. The combination was determined by linearly weighting each component by the time series mean value in each voxel for that component (Glover and Law, 2001). The spiral-out time series was obtained from the same scan data set by simply extracting that component and writing a new file. It was previously shown that introducing the spiral-in trajectory before the spiral-out readout did not increase the physiological noise or reduce the BOLD signal in the latter (Glover and Law, 2001). Both time series thus obtained for each scan were then subjected to the

same postprocessing stream so that intrasubject comparisons could be made for the effect of acquisition sequence type without concern for motion or cognitive adaptation.

Data analysis

The metrics used to compare the effects of sequence (spiral-io vs. spiral-out) and field strength (1.5 vs. 3.0 T) included voxel dropout counts and extent of activation (number of activated voxels and Z scores) in ROIs specific for each task for each subject. In addition, a global analysis of activation volume was performed for the two time series.

Preprocessing and individual statistical analyses

Image preprocessing and statistical analyses were performed using SPM99 (Wellcome Department of Cognitive Neurology). Functional volumes were realigned to the first volume in the time series to correct for motion. A mean T2*-weighted volume was computed during realignment, and the T2-weighted anatomical volume was coregistered to this mean functional volume. The functional volumes were then smoothed with a 7-mm isotropic Gaussian kernel.

For individual subjects, differences between conditions in each task (e.g., novel and repeated blocks in the scenes task) were assessed using the general linear model (Friston et al., 1995). Regressor functions were constructed by modeling stimulus-related activation as a delayed boxcar function convolved with a synthetic hemodynamic response function. Individual subject data were then analyzed using a fixed effects model (Friston et al., 1994), and linear contrasts were performed to generate a SPM{t} map representing differences in brain activation between the conditions for each task: novel > repeated blocks for the scenes task, experimental > control blocks in the letters task, and negative > neutral blocks in both the photos and film tasks.

ROI definition and analyses

Regions of interest for the LPFC (left superior, middle, and inferior frontal gyri; letters task), MTL (scenes task), and amygdala (photos and film tasks) were generated from the Talairach and Tournoux coordinates (Talairach and Tournoux, 1988) defining these regions. These coordinates were then transformed into the standard space of the Montreal Neurological Institute (MNI) series (Brett, 2000). An additional ROI for the VMPFC (photos and film tasks) was defined by outlining the region just below the genu of the corpus callosum and midway across the ventral aspect of the orbital frontal cortex on the SPM canonical image in MNI space. All regions were then coregistered to each individual's T2 in-plane anatomy.

For each ROI, the percentage of voxels susceptible to signal dropout was calculated for each subject for both fields and both spiral sequences. A voxel was determined to be susceptible to signal dropout if its intensity was below the threshold determined by the SPM99 masking procedure. This procedure first eliminates all voxels in an image whose T2* intensity is less than one-eighth of the global mean of the entire image. The mean of the remaining voxels is calculated and used as a second threshold, and all voxels with intensities below this mean are also eliminated. Using these calculations of percentage signal dropout, separate Repeated Measures ANOVAs were performed for each ROI with field strength (1.5 and 3 T) and

spiral sequence (spiral-io, spiral-out) as repeated factors and subjects as a random factor. Additional planned comparisons were also performed to assess the specific differences between the following conditions: 3 T spiral-io and 3 T spiral-out; 1.5 T spiral-io and 1.5 T spiral-out; 3 T spiral-io and 1.5 T spiral-out; 3 T spiral-out and 1.5 T spiral-out.

Additional ROI analyses were performed to assess the extent of activation in each task-specific region for each subject. For the linear contrasts specific to each task, the percentage of voxels that reached a specified threshold ($P < 0.05$, except $P < 0.001$ for scenes task, and $P < 0.10$ for photos task, all uncorrected) within an ROI were calculated for each subject for all field by spiral sequence combinations. Similar to the analyses for signal dropout, separate Repeated Measures ANOVAs were performed for the percentage of activated voxels within each ROI. Field strength (1.5 and 3 T) and spiral sequence (spiral-io, spiral-out) served as repeated factors and subjects as a random factor. Additional planned comparisons were also performed to assess the specific differences in the extent of activation between the following conditions: 3 T spiral-io and 3 T spiral-out; 1.5 T spiral-io and 1.5 T spiral-out; 3 T spiral-io and 1.5 T spiral-out; 3 T spiral-out and 1.5 T spiral-out.

Global analysis

The extent of global brain activation was also measured on an individual subject basis for each task. For the linear contrasts specific to each task, the percentage of voxels within the entire brain that reached a threshold of $P < 0.001$ uncorrected were calculated for each subject for all fields by spiral sequence combinations. Separate Repeated Measures ANOVAs were performed for the global percentage of activated voxels for each task with field strength (1.5 and 3 T) and spiral sequence (spiral-io, spiral-out) as repeated factors and subjects as a random factor. Additional planned comparisons were again calculated to examine specific differences between the following conditions for each task: 3 T spiral-io and 3 T spiral-out; 1.5 T spiral-io and 1.5 T spiral-out; 3 T spiral-io and 1.5 T spiral-out; 3 T spiral-out and 1.5 T spiral-out.

Group statistical analysis

A group analysis was performed by spatially normalizing the T2-weighted anatomical volume into common stereotactic space (Talairach and Tournoux, 1988) using a standard template brain from the MNI series. The spatial transformations calculated during the normalization of the anatomical volume were then used to normalize the realigned functional volumes. After normalization, the functional volumes were resampled to 2-mm^3 voxels and smoothed with a 7-mm isotropic Gaussian kernel. Normalized individual subject data were then analyzed using a fixed effects model (Friston et al., 1994), and linear contrasts were performed to generate a SPM{t} map representing differences in brain activation between the conditions for each task: novel > repeated blocks for the scenes task, experimental > control blocks in the letters task, and negative > neutral blocks in both the photos and film tasks. Contrast images generated in the individual subject analysis using the spatially normalized data were then analyzed across subjects using a mixed-effects general linear model, treating subjects as random effect allowing for population inference (Holmes and Friston, 1998).

Z score analysis

From the 3-T spiral-io group analysis, voxels that reached a threshold of $P < 0.001$ uncorrected were identified within the ROIs for each task. These voxels were treated as functional ROIs and the corresponding Z scores were extracted for each field by sequence combination. To examine whether the distribution of Z scores were different across the field by sequence combinations, Kolmogorov–Smirnov (K–S) statistics were calculated for the following pairwise comparisons: 3 T spiral-io and 3 T spiral-out; 1.5 T spiral-io and 1.5 T spiral-out; 3 T spiral-io and 1.5 T spiral-out; 3 T spiral-out and 1.5 T spiral-out.

Results

Regional signal dropout

Fig. 1A displays the average T2*-weighted time series images for one subject highlighting signal dropout in task-specific ROIs. The results averaged over all subjects are summarized in Fig. 1B for each of the four regions pertaining to the cognitive tasks, and quantitative detail is provided in Table 1. Repeated Measures ANOVAs demonstrated a significant main effect of spiral sequence in all ROIs, revealing significantly greater signal dropout for the spiral-out sequence relative to spiral-io sequence regardless of field strength (Table 1). In addition, a main effect of field strength was observable for the VMPFC and amygdala (photos task) with trends toward significance for the LPFC and amygdala (film task). For these regions, signal dropout was significantly greater for the 3-T data relative to the 1.5-T data regardless of spiral sequence. A significant interaction between field strength and spiral sequence was also observable in all regions. As shown in Fig. 1B, there was a significant increase in dropout for all regions at 3 vs. 1.5 T using the spiral-out sequence, while the dropout was reduced (in LPFC, VMPFC, and amygdala) or mitigated entirely (in MTL) with the spiral-io sequence (Table 1). Thus, the spiral-io sequence provides substantially reduced signal dropout at 3 T and can eliminate the signal dropout disadvantage of higher fields observed in frontal, medial temporal, and amygdala regions with spiral-out.

Regional activation volumes

Results for the ROI analysis of task-related activation are presented in Fig. 2 and Table 2. The comparisons of activation maps for each ROI are shown in Fig. 2A, with summary plots in Fig. 2B. Repeated Measures ANOVAs revealed a significant main effect of spiral sequence in MTL, LPFC, VMPFC (photo task), and a trend in the amygdala (film task). For these regions, the percent of activated voxels within a region was increased for spiral-io relative to spiral-out regardless of field strength. The MTL and VMPFC (film task) also demonstrated significant differences in regional activation volumes with greater activation for the 3-T acquisition vs. the 1.5-T acquisition. A trend for this main effect of field strength was also observable in LPFC during the letters task.

Trends for the interaction between field strength and spiral sequence were observable in all regions. Within the MTL, significantly more activation during the scenes task was observed for the 3 T spiral-io sequence relative to the 1.5 T spiral-io sequence, and this difference was larger than the one between the 3 T spiral-out and 1.5 T spiral-out sequences (Table 2). Similar patterns of results were observed in the LPFC for the letters task, and in the VMPFC

and amygdala for the film task. Thus, the spiral-io acquisition provided increased regional activation volumes in all regions at 3 T relative to that at 1.5 T, in contrast to the spiral-out acquisition in which regional activation volumes were reduced or eliminated at the higher field strength.

Global activation volumes

Activation maps are shown in Fig. 3A for one subject performing the scenes task, with the ROI used for the regional calculations overlaid. For this subject, global activation (i.e., not limited to the anatomically constrained activation ROIs) is much greater at 3 T with the spiral-io sequence than at 1.5 T using spiral-io and at 3 T with conventional spiral-out. Global analysis of activation volumes across all subjects revealed a significant main effect for spiral-io vs. spiral-out for the letters and film task as well as a trend for significance in the photo task (Fig. 3B and Table 3), but not for the scenes task. The main effect of field strength was also either significant or had a strong trend for the letters, film, and photos tasks. The letters and photos tasks demonstrated additional interactions between field strength and spiral sequence. For these regions, global activation volumes were increased at 3 T relative to scans at 1.5 T, but these benefits were greater when using the spiral-io sequence. A trend for the same pattern was also observable in the film task.

Z score analyses

Fig. 4 shows histograms of the Z scores in LPFC for the letters task, demonstrating higher mean activation scores for spiral-io vs. spiral-out for both the 3-T and the 1.5-T scans. The K–S tests revealed that comparisons of the Z score distributions in LPFC for the letters task (1.5 T spiral-io vs. 1.5 T spiral-out; 3 T spiral-io vs. 3 T spiral-out; 3 T spiral-io vs. 1.5 T spiral-io; and 3 T spiral-out vs. 1.5 T spiral-out) were significant (Table 4). Analyses of the Z score distributions for activated regions in the MTL, VMPFC, and amygdala demonstrated similar patterns of results except that none of these regions demonstrated a significant difference in Z scores for 1.5 T spiral-io vs. 1.5 T spiral-out. Thus, within the chosen ROIs, the activation Z scores were greater for the 3-T scans relative to those at 1.5 T regardless of sequence. At 3 T, additional increases in Z scores were observed for the spiral-io relative to the spiral-out sequence in all regions. In the LPFC, the increase in Z scores for the spiral-io sequence was also observable at 1.5 T.

Discussion and summary

Many approaches have been introduced for reduction of the deleterious effects of SFGs, including z-shim methods (Constable and Spencer, 1999; Glover, 1999a; Yang et al., 1997, 1998), 3D acquisitions (Lai and Glover, 1998), and tailored RF pulses (Glover and Lai, 1998a; Stenger et al., 2000). However, each of these methods has disadvantages in terms of either increased scan time, complexity of setup and/or processing, or in delivering only modest benefit. By contrast, the spiral-io method does not increase the scan time per volume and requires only simple postprocessing of the time series data.

In this study, ROIs were defined anatomically with relevance to the four tasks employed, and signal dropout and activation were quantitated within the ROIs. With the conventional

spiral-out sequence, it was found that significant increases in signal dropout were observed at 3 vs. 1.5 T, as has been shown previously (Krasnow et al., 2003). However, use of the spiral-io sequence resulted in significantly reduced signal dropout in all ROIs at both field strengths. In fact, in MTL, the spiral-io sequence resulted in reduced dropout at 3 vs. 1.5 T (Fig. 1B). The reason for this reduction may be a consequence of the particular choice of ROIs, but in any case the spiral-io sequence clearly recovers lost signal relative to spiral-out as shown in Fig. 1A and Table 1.

Analysis of activation volumes in the task-specific ROIs demonstrated increased activation volumes for the 3-T acquisitions relative to those at 1.5 T in all regions, excluding the amygdala with the spiral-out sequence, consistent with a previous study (Krasnow et al., 2003). In addition, regional activation volumes were increased for the spiral-io sequence relative to spiral-out for all ROIs. There was a trend for the effects of spiral-io to be larger on the 3-T than on the 1.5-T magnet in all regions. In the case of amygdala activation during the film task, activation seen at 1.5 T was not observable at 3 T with the conventional spiral-out method, but was recovered using the spiral-io acquisition method. Additional Z score analyses were consistent with the findings from the regional activation analyses, demonstrating greater mean Z scores for 3 T spiral-io compared to 1.5 T spiral-io, and greater Z scores for 3 T spiral-io relative to 3 T spiral-out in all regions. Thus, the spiral-io method was found to mitigate the effects of SFGs and eliminate BOLD signal losses in amygdala and other regions when compared to the spiral-out sequence at 3 T.

While substantial benefits were shown in ROIs chosen for the tasks utilized here, other choices of tasks or even different ROIs with these tasks might have demonstrated even more regional benefit as shown for the subject in Fig. 3A. Increased global activation volumes were seen with the spiral-io sequence vs. spiral-out methods in three of the tasks chosen (Fig. 3B), although no benefit was observed for the scenes task when averaged over all subjects at either field. Note that a relatively stringent threshold for global activation was chosen ($P < 0.001$), and this reduced the apparent activation. In fact, anecdotal results in our laboratory using many other tasks have shown substantially increased global activation with the spiral-io sequence in a wide range of cortical regions including magnetically uniform brain areas at both 1.5 and 3 T. The advantages of spiral-io in uniform brain regions derive from longer total readout time of the dual trajectory, which typically provides an SNR increase of at least 30% (Glover and Law, 2001). That in turn can result in greater BOLD CNR in cortical regions supporting the neural activation. Of course, if the spiral-in and spiral-out images are simply averaged instead of combined adaptively as here, the spiral-out image may degrade SNR from the spiral-in image in nonuniform regions (Glover and Thomason, in press).

In principle, acquisition of the spiral-in image does not change the sequence timing as long as the readout fits between the end of the RF pulse and TE, where the spiral-out readout begins. However, there are two factors that can increase the acquisition time per slice. The first is that while the spiral-out trajectory can utilize a short, nonchemical-shift-selective RF excitation pulse because the fat signal (with its short T2*) decays away by the beginning of the readout, the spiral-in acquisition is distorted by the off-resonant lipid signals that still have significant intensity near the beginning of the trajectory, and thus suppression of these

signals is required. Either water-selective excitation, as employed here, or fat saturation must be utilized, and either technique requires a longer RF pulse than simple spatial selection. With the functional acquisition parameters used in this study, the spiral-io sequence requires about 65 ms/slice, while a conventional spiral-out sequence without fat suppression has a duration of only 59 ms/slice; that is, 10% less. The second factor is that the spiral-io sequence dissipates twice the readout gradient power and may incur duty cycle limitations from either the gradient amplifiers or gradient coils that reduce the number of slices per unit time that can be acquired. An additional, nontiming-related disadvantage is that the spiral-io trajectory is acoustically louder than the spiral-out acquisition, which may be a consideration for some studies.

The spiral-in and spiral-out images were combined to form the spiral-io time series using linear weighting based on the mean voxel intensities for each component (-in and -out) time series, as introduced previously (Glover and Law, 2001). However, investigations of other combination strategies based on statistical weighting of the two components have demonstrated even greater gains for spiral-io (Glover and Thomason, in press).

In summary, this study has demonstrated that spiral-io methods recover more raw signal as well as BOLD contrast in regions affected by SFGs relative to conventional spiral-out acquisitions, and the advantages are greater at 3 T than at 1.5 T. For example, it was found that activation in amygdala observed at 1.5 T disappeared at 3 T with the conventional sequence, but the spiral-io method provided gains in activation in amygdala similar to those observed in other regions for the higher field strength. Moreover, in addition to eliminating or significantly reducing the dropout of signal and increasing the activation and Z scores in such regions, spiral-io also provides significant benefits in magnetically uniform brain regions. Thus, despite slightly reduced sequence timing efficiency (slices/s) and increased acoustic noise, the spiral-io method appears to largely eliminate the deleterious effects of higher field and may contribute to improved acquisitions in frontal and temporal brain regions traditionally compromised by susceptibility induced gradients.

Acknowledgments

References

Bandettini PA, Wong EC, Hinks RS, Tikofsky RS, Hyde JS, 1992. Time course EPI of human brain function during task activation. Magn. Reson. Med. 25 (2), 390–397. [PubMed: 1614324]

Brett M, 2000. The MNI Brain and the Talairach Atlas. http://www.mrc-cbu.cam.ac.uk/Imaging/mnispace.html.

Constable R, Spencer D, 1999. Composite image formation in Z-shimmed functional MR imaging. Magn. Reson. Med. 42, 110–117. [PubMed: 10398956]

Friston KJ, Jezzard P, Turner R, 1994. Analysis of functional MRI time-series. Hum. Brain Mapp. 1, 153–171.

Friston KJ, Holmes AP, Poline JB, Grasby PJ, Williams SC, Frackowiak RS, Turner R, 1995. Analysis of fMRI time-series revisited. NeuroImage 2 (1), 45–53. [PubMed: 9343589]

Gabrieli JDE, Brewer JB, Desmond JE, Glover GH, 1997. Separate neural bases of two fundamental memory processes in the human medial temporal lobe. Science 276 (5310), 264–266. [PubMed: 9092477]

Gati JS, Menon RS, Ugurbil K, Rutt BK, 1997. Experimental determination of the BOLD field strength dependence in vessels and tissue. Magn. Reson. Med. 38 (2), 296–302. [PubMed: 9256111]

Glover G, 1999a. 3D Z-Shim method for reduction of susceptibility effects in BOLD fMRI. Magn. Reson. Med. 42, 290–299. [PubMed: 10440954]

Glover G, 1999b. Simple analytic spiral k-space algorithm. Magn. Reson. Med. 42, 412–415. [PubMed: 10440968]

Glover G, Lai S, 1998a. Reduction of susceptibility effects in BOLD fMRI using tailored RF pulses. Proc. Sixth Annual Meeting of the ISMRM, Sydney.

Glover GH, Lai S, 1998b. Self-navigated spiral fMRI: interleaved versus single-shot. Magn. Reson. Med. 39 (3), 361–368. [PubMed: 9498591]

Glover GH, Law CS, 2001. Spiral-in/out BOLD fMRI for increased SNR and reduced susceptibility artifacts. Magn. Reson. Med. 46 (3), 515–522. [PubMed: 11550244]

Glover GH, Thomason ME, 2003. Improved combination of spiral-in/out images for BOLD fMRI. Magn. Reson. Med. (in press).

Gross JJ, 1998. Antecedent and response-focused emotion regulation: divergent consequences for experience, expression and physiology. J. Pers. Soc. Psychol. 74 (1), 224–237. [PubMed: 9457784]

Holmes AP, Friston KJ, 1998. Generalizability, random effects, and population inference. NeuroImage 7, 754.

Kim DH, Adalsteinsson E, Glover G, Spielman D, 2002. Regularized higher-order in vivo shimming. Magn. Reson. Med. 48, 715–722. [PubMed: 12353290]

King KF, Ganin A, Zhou XJ, Bernstein MA, 1999. Concomitant gradient field effects in spiral scans. Magn. Reson. Med. 41 (1), 103–112. [PubMed: 10025617]

Krasnow B, Tamm L, Grecius M, Yang T, Glover G, Reiss A, Menon V, 2003. Comparison of fMRI activation at 3 T and 1.5 T during perceptual, cognitive and affective processing. NeuroImage 18, 813–826. [PubMed: 12725758]

Kruger G, Glover G, 2001. The physiological noise in oxygen-sensitive magnetic resonance imaging. Magn. Reson. Med. 46, 631–637. [PubMed: 11590638]

Kruger G, Kastrup A, Glover G, 2001. Neuroimaging at 1.5 T and 3.0 T: comparison of oxygen-sensitive magnetic resonance imaging. Magn. Reson. Med. 45, 594–604.

Kwong KK, Belliveau JW, Chesler DA, et al. , 1992. Dynamic magnetic resonance imaging of human brain activity during primary sensory stimulation. Proc. Natl. Acad. Sci. U. S. A. 89 (12), 5675–5679. [PubMed: 1608978]

Lai S, Glover G, 1998. Three-Dimensional Spiral fMRI technique: a comparison with 2D spiral acquisition. Magn. Reson. Med. 39, 68–78. [PubMed: 9438439]

Lane RD, Reiman EM, Ahern GL, Schwartz GE, Davidson RJ, 1997. Neuroanatomical correlates of happiness, sadness, and disgust. Am. J. Psychiatry 154 (7), 926–933. [PubMed: 9210742]

Lang P, Greenwald M, Bradley M, Hamm A, 1993. Looking at pictures: affective, facial, visceral, and behavioral reactions. Psychophysiology 30, 261–273. [PubMed: 8497555]

Meyer CH, Pauly JM, Macovski A, Nishimura DG, 1990. Simultaneous spatial and spectral selective excitation. Magn. Reson. Med. 15 (2), 287–304. [PubMed: 2392053]

Ochsner KN, Feldman Barrett L, 2001. A multiprocess perspective on the neuroscience of emotion. In: Mayne TJ, Bonanno GA (Eds.), Emotions: Current Issues and Future Directions. The Guilford, New York, NY, pp. 38–81.

Ochsner KN, Bunge SA, Gross JJ, Gabrieli JDE, 2002. Rethinking feelings: an fMRI study of the cognitive regulation of emotion. J. Cogn. Neurosci. 14, 1215–1299. [PubMed: 12495527]

Ogawa S, Lee TM, Kay AR, Tank DW, 1990. Brain magnetic resonance imaging with contrast dependent on blood oxygenation. Proc. Natl. Acad. Sci. U. S. A. 87 (24), 9868–9872. [PubMed: 2124706]

Smith EE, Jonides J, 1997. Working memory: a view from neuroimaging. Cogn. Psychol. 33, 5–42. [PubMed: 9212720]

Stenger VA, Boada FE, Noll DC, 2000. Three-dimensional tailored RF pulses for the reduction of susceptibility artifacts in T2*-weighted functional MRI. Magn. Reson. Med. 44, 525–531. [PubMed: 11025507]

Stern CE, Corkin S, Gonzalez RG, et al. , 1996. The hippocampal formation participates in novel picture encoding: evidence from functional magnetic resonance imaging. Proc. Natl. Acad. Sci. U. S. A. 93 (16), 8660–8665. [PubMed: 8710927]

Talairach J, Tournoux P, 1988. Co-planar Stereotactic Atlas of the Human Brain. Thieme Medical Publishers Inc., New York.

Turner R, Jezzard P, Wen H, Kwong KK, Le BD, Zeffiro T, Balaban RS, 1993. Functional mapping of the human visual cortex at 4 and 1.5 tesla using deoxygenation contrast EPI. Magn. Reson. Med. 29 (2), 277–279. [PubMed: 8429797]

Yang QX, Dardzinski BJ, Li S, Eslinger PJ, Smith MB, 1997. Multi-gradient echo with susceptibility inhomogeneity compensation (MGESIC): demonstration of fMRI in the olfactory cortex at 3.0 T. Magn. Reson. Med. 37 (3), 331–335. [PubMed: 9055220]

Yang QX, Williams GD, Demeure RJ, Mosher TJ, Smith MB, 1998. Removal of local field gradient artifacts in T2*-weighted images at high fields by gradient-echo slice excitation profile imaging. Magn. Reson. Med. 39 (3), 402–409. [PubMed: 9498596]

Yang Y, Wen H, Mattay VS, Balaban RS, Frank JA, Duyn JH, 1999. Comparison of 3D BOLD functional MRI with spiral acquisition at 1.5 and 4.0 T. NeuroImage 9 (4), 446–451. [PubMed: 10191173]
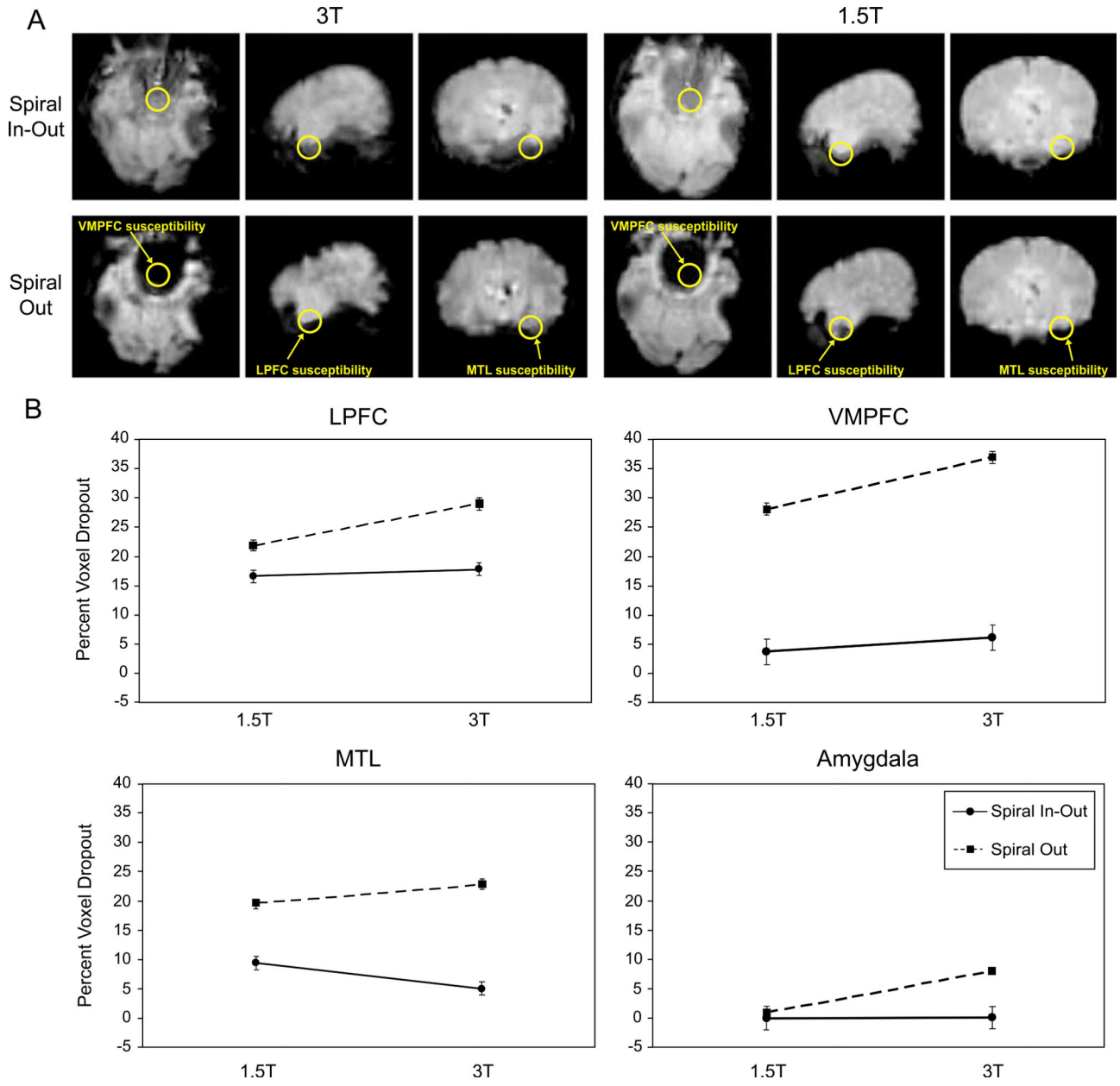
Fig. 1.
(A) Example of the comparison of T2* weighted images from one subject, showing ROIs used for the dropout analysis in regions associated with the tasks performed. ROIs for amygdala are similar in location to those for MTL but are more anterior and not shown for clarity. (B) Signal dropout for each ROI averaged over all subjects. Dropout is greater in all regions at 3 vs. 1.5 T for the spiral-out sequence. Dropout for the spiral-io sequence is significantly reduced vs. spiral-out at 3 T and is either the same or significantly reduced (in MTL) at 1.5 T.
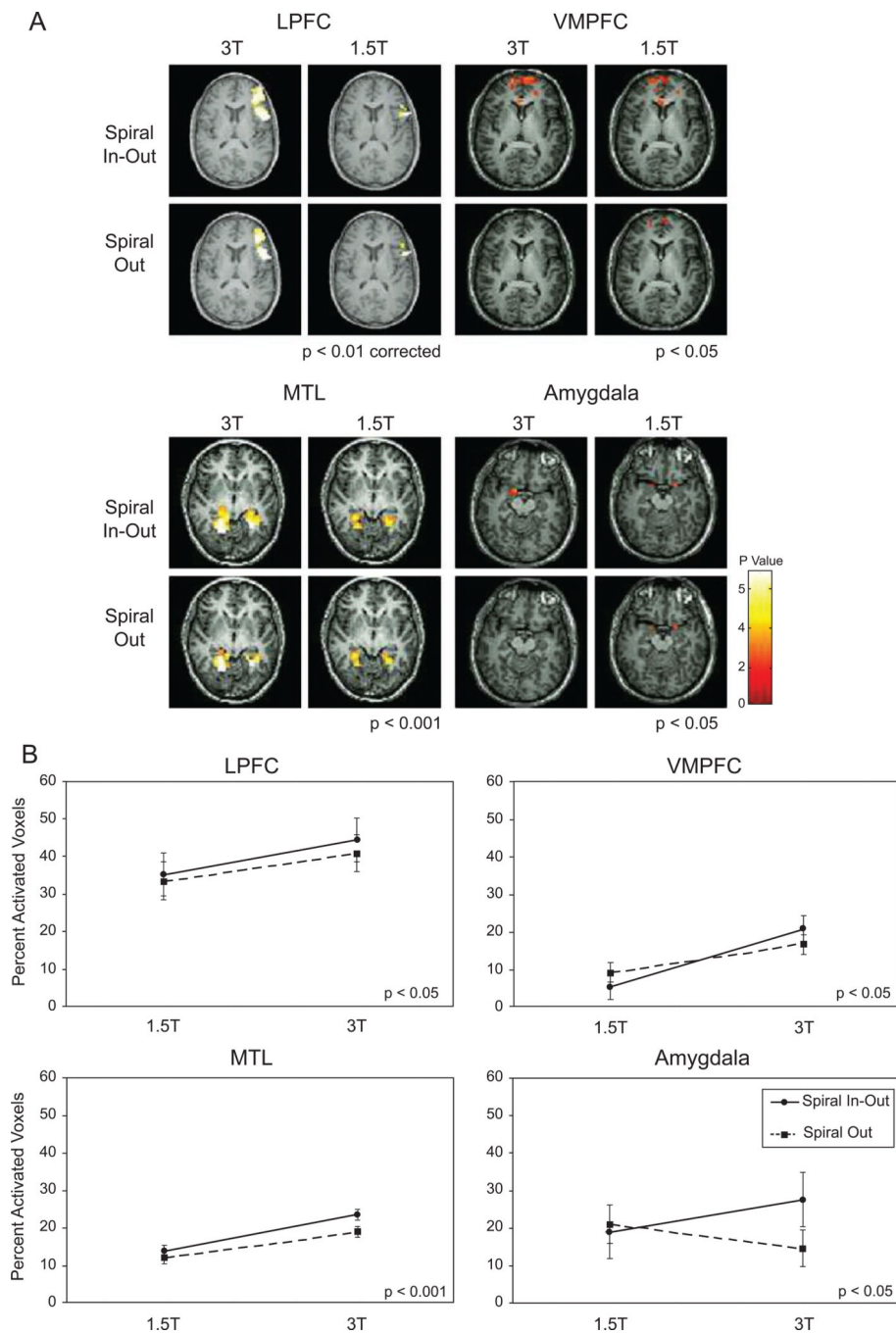
Fig. 2.
(A) Example of single-subject activation maps. Activation seen in amygdala at 1.5 T is lost at 3 T with spiral-out, but is recovered and greater at 3 T with spiral-io. (B) Activation volumes as a percentage of ROI volume, showing nonsignificant differences for sequence type at 1.5 T, increased activation extent for all regions with spiral-io at 3 T over 1.5 T and less gains (loss in amygdala) with spiral-out. For all subjects, the spiral-io sequence more than mitigated the activation volume loss in amygdala with the conventional spiral sequence at 3 T. The film task was used for the VMPFC and amygdala maps and plots.

Fig. 3.
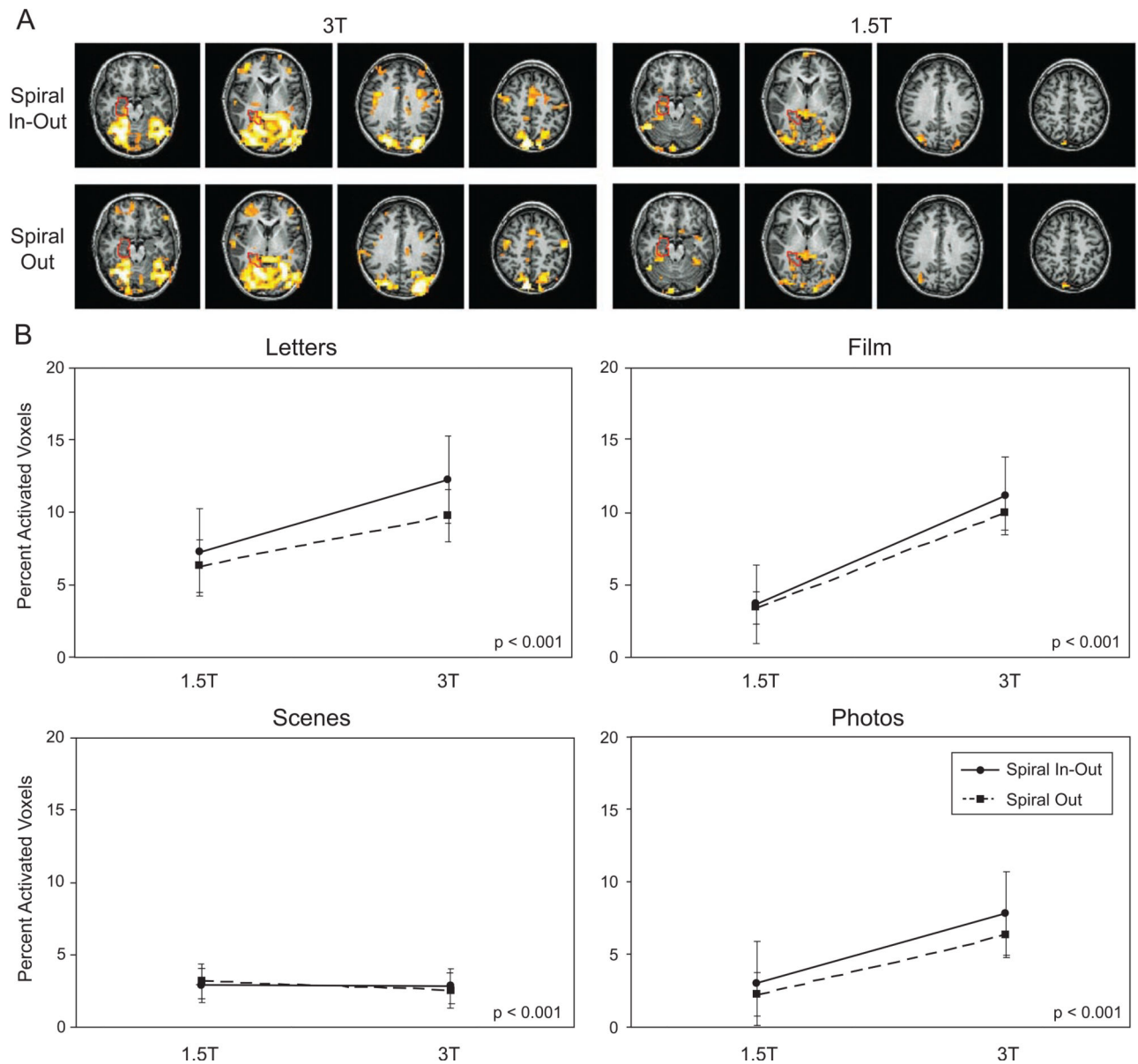(A) Example of single-subject activation maps displayed at a threshold of *P* < 0.001 in four selected slices for the scenes task, showing the MTL ROI used for quantitation. The global advantage of the spiral-io sequence and 3-T field strength is apparent for this subject. (B) Plots of global activation volumes as a percent of brain volume for all subjects, demonstrating advantage of spiral-io in three of the tasks.

Fig. 4.
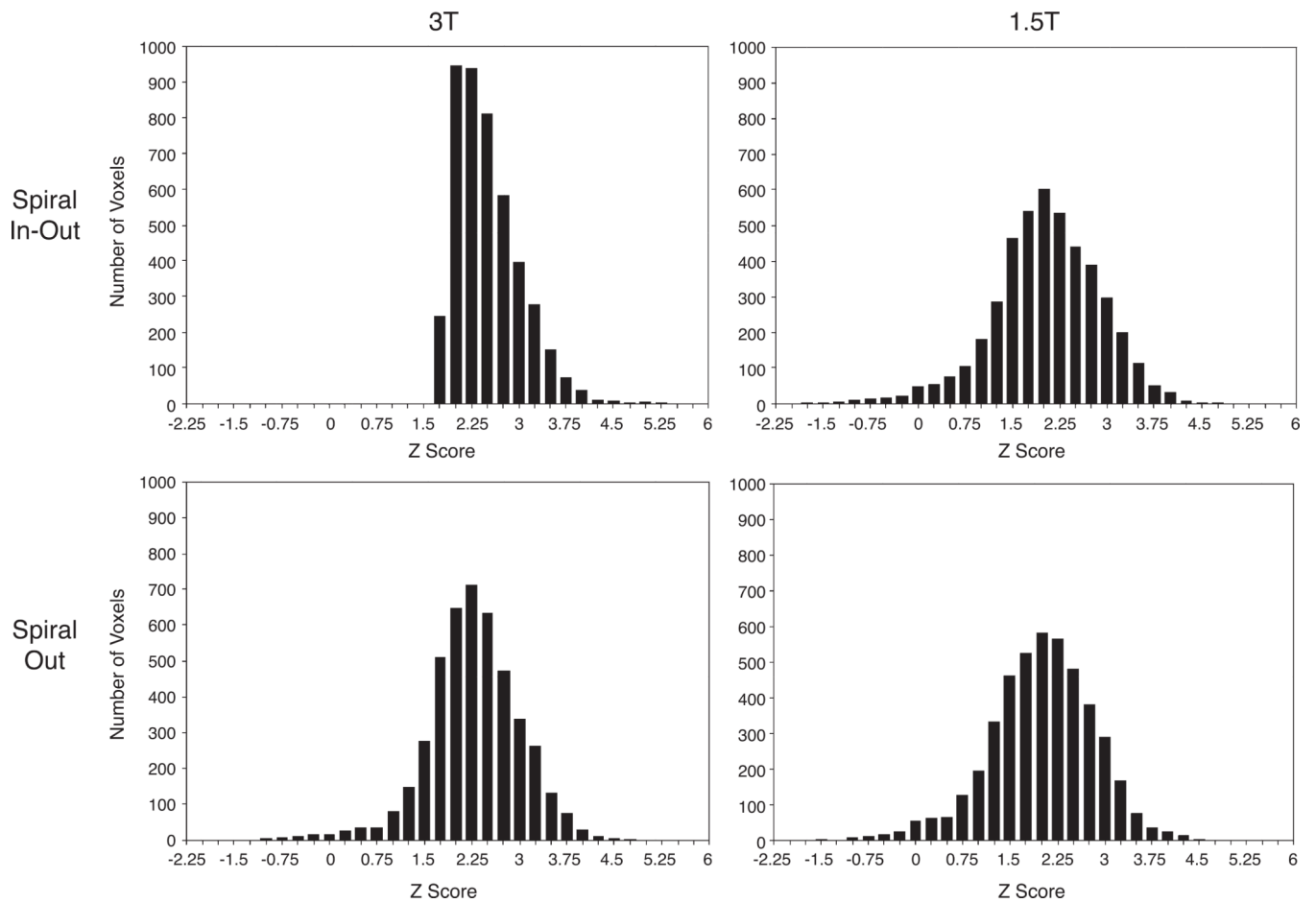Histograms of Z scores comparing sequence and field strength in LPFC for the letters task. The 3 T spiral-io distribution is qualitatively different from that for spiral-out with higher mean values (2.38 vs. 2.15) and skew towards greater Z scores, while at 1.5 T, the mean Z scores for spiral-io and spiral-out are 1.91 vs. 1.87, respectively. K–S statistics revealed significant differences between all distributions.

Table 1

Percent dropped voxels (SEM)

Field/F/t	Comparison	LPFC	MTL	VMPFC (film)	VMPFC (photo)	Amygdala (film)	Amygdala (photo)
3 T	spiral-io	17.81 (1.55)	5.04 (0.91)	6.18 (1.06)	6.14 (1.20)	0.16 (0.16)	0.20 (0.20)
	spiral-out	28.99 (1.32)	22.88 (1.24)	36.86 (2.39)	39.42 (3.03)	8.05 (3.88)	17.54 (7.47)
1.5 T	spiral-io	16.61 (1.57)	9.41 (1.09)	3.81 (0.97)	3.60 (0.88)	0.00 (0.00)	0.00 (0.00)
	spiral-out	21.91 (1.57)	19.59 (1.19)	28.09 (2.42)	27.46 (2.87)	0.97 (0.43)	0.40 (0.40)
F(P value)	3 T	3.58 (0.11)	0.32 (0.59)	26.12 (0.00)*	31.29 (0.00)*	3.19 (0.11)	5.55 (0.05)*
	spiral-io	142.86 (0.00)*	473.33 (0.00)*	252.60 (0.00)*	202.30 (0.00)*	5.60 (0.05)*	5.44 (0.05)*
	3 T*spiral-io	99.54 (0.00)*	161.02 (0.00)*	12.13 (0.01)*	33.46 (0.00)*	2.93 (0.13)	5.20 (0.05)*
t score (P value)	spiral-io (3 T)–spiral-out (3 T)	12.96 (0.00)*	19.35 (0.00)*	17.04 (0.00)*	1.87 (0.10)	2.04 (0.05)*	2.31 (0.05)*
	spiral-io (1.5 T)–spiral-out (1.5 T)	8.60 (0.00)*	25.36 (0.00)*	11.54 (0.00)*	2.50 (0.04)*	2.26 (0.08)	1.00 (0.35)
	spiral-io (3 T)–spiral-io (1.5 T)	0.50 (0.64)	3.87 (0.01)*	4.50 (0.01)*	1.31 (0.23)	1.00 (0.35)	1.00 (0.35)
	spiral-out (3 T)–spiral-out (1.5 T)	3.57 (0.01)*	3.96 (0.01)*	4.51 (0.01)*	1.77 (0.12)	1.75 (0.12)	2.32 (0.05)*

Table 2

Percent activated voxels (SEM)[†]

Field/F/t	Comparison	LPFC	MTL	VMPFC (film)	VMPFC (photo)	Amygdala (film)	Amygdala (photo)
3 T	spiral-io	44.39 (6.24)	23.66 (2.31)	20.98 (5.42)	47.65 (7.85)	27.55 (7.81)	54.66 (12.66)
	spiral-out	40.31 (5.16)	18.93 (2.22)	16.83 (3.28)	40.62 (8.56)	14.65 (2.72)	55.27 (12.48)
1.5 T	spiral-io	35.20 (6.32)	13.88 (1.59)	5.39 (1.88)	34.86 (7.38)	19.00 (7.42)	40.75 (11.88)
	spiral-out	33.42 (5.74)	12.06 (1.63)	9.23 (3.65)	27.15 (6.90)	21.00 (7.90)	42.20 (10.94)
F (P value)	3 T	3.09 (0.13)	9.823 (0.02)*	7.29 (0.03)*	2.51 (0.16)	0.06 (0.82)	1.34 (0.28)
	spiral-io	8.24 (0.02)*	32.93 (0.001)*	0.003 (0.96)	14.86 (0.01)*	4.07 (0.08)	0.08 (0.78)
	3 T*spiral-io	3.34 (0.12)	5.13 (0.06)	4.59 (0.07)	0.01 (0.91)	4.74 (0.07)	0.01 (0.91)
t score (P value)	spiral-io (3 T)–spiral-out (3 T)	2.77 (0.03)*	4.14 (0.006)*	1.17 (0.28)	1.87 (0.10)	2.16 (0.07)	0.15 (0.89)
	spiral-io (1.5 T)–spiral-out (1.5 T)	2.67 (0.04)*	4.45 (0.004)*	1.34 (0.22)	2.50 (0.04)*	1.27 (0.24)	0.25 (0.81)
	spiral-io (3 T)–spiral-io (1.5 T)	1.85 (0.11)	3.53 (0.01)*	3.31 (0.01)*	1.31 (0.23)	1.69 (0.14)	0.98 (0.36)
	spiral-out (3 T)–spiral-out (1.5 T)	1.64 (0.15)	2.55 (0.04)*	1.64 (0.15)	1.77 (0.12)	1.01 (0.35)	1.32 (0.23)

[†]$P < 0.05$, except $P < 0.001$ (MTL), $P < 0.10$ (photo task).

Table 3

Global percent activated voxels (SEM)[†]

Field/*F*/*t*	Comparison	Letters	Scenes	Film	Photos
3 T	spiral-io	12.25 (3.40)	2.81 (1.21)	11.10 (2.87)	7.82 (3.41)
	spiral-out	9.79 (2.64)	2.57 (1.16)	9.89 (2.46)	6.31 (2.77)
1.5 T	spiral-io	7.27 (1.99)	2.94 (1.16)	3.65 (1.10)	3.00 (1.77)
	spiral-out	6.28 (1.65)	3.17 (1.21)	3.40 (1.02)	2.25 (1.26)
F (*P* value)	3 T	3.48 (0.11)	0.05 (0.83)	8.88 (0.02)*	6.33 (0.04)*
	spiral-io	10.61 (0.02)*	0.00 (0.97)	6.19 (0.04)*	3.85 (0.09)
	3 T*spiral-io	6.02 (0.05)*	2.60 (0.16)	2.55 (0.15)	5.22 (0.05)*
t score (*P* value)	spiral-io (3 T)–spiral-out (3 T)	3.15 (0.02)*	–0.89 (0.41)	2.08 (0.08)	2.27 (0.06)
	spiral-io (1.5 T)–spiral-out (1.5 T)	2.74 (0.03)*	2.39 (0.05)*	2.04 (0.08)	1.43 (0.20)
	spiral-io (3 T)–spiral-io (1.5 T)	1.95 (0.10)	0.07 (0.94)	2.97 (0.02)*	2.57 (0.04)*
	spiral-out (3 T)–spiral-out (1.5 T)	1.76 (0.13)	0.37 (0.72)	2.96 (0.02)*	2.44 (0.04)*

[†]$P < 0.001$, uncorrected for all.

Table 4

K – S statistics for *Z* score distribution [†]

Sequence/K – S stat	Value/comparison	Letters	Scenes	Film	Photos
3 T spiral-io	mean (SEM)	2.38 (0.008)	3.51 (0.011)	2.00 (0.023)	1.49 (0.042)
	kurtosis	4.18	0.58	2.60	2.92
3 T spiral-out	mean (SEM)	2.15 (0.011)	3.03 (0.028)	1.61 (0.059)	0.79 (0.121)
	kurtosis	4.63	14.9	4.70	2.08
1.5 T spiral-io	mean (SEM)	1.91 (0.013)	3.48 (0.014)	2.38 (0.45)	−0.07 (0.110)
	kurtosis	4.05	1.17	2.88	2.08
1.5 T spiral-out	mean (SEM)	1.87 (0.012)	3.47	2.34 (0.041)	0.22 (0.010)
	kurtosis	3.84	−0.22	2.66	1.67
K – S stat (*P* value)	spiral-io (3 T)–spiral-out (3 T)	0.225 (0.00)*	0.533 (0.00)*	0.632 (0.00)*	0.727 (0.00)*
	spiral-io (1.5 T)–spiral-out (1.5 T)	0.029 (0.04)*	0.057 (0.12)	0.132 (0.26)	0.318 (0.17)
	spiral-io (3 T)–spiral-io (1.5 T)	0.372 (0.00)*	0.160 (0.00)*	0.474 (0.00)*	1.00 (0.00)*
	spiral-out (3 T)–spiral-out (1.5 T)	0.163 (0.00)*	0.028 (0.00)*	0.623 (0.00)*	0.409 (0.04)*

[†] $a < 0.0125$.